

# Aerodynamics Study of Automobile Car Ahmed Body using CFD Simulation to Predict the Drag Coefficient and Down Forces

Mrs. Ashwini A Landge<sup>1</sup> Prof. D. D. Palande<sup>2</sup>

<sup>1</sup>Student <sup>2</sup>Associate Professor

<sup>1,2</sup>Department of Mechanical Engineering

<sup>1,2</sup>Pune University, MCERC, Nashik-423101, India

**Abstract**— The Ahmed body is a simplified car used in automotive industry to investigate the influence of the flow structure on the drag. The external aerodynamics of the car determines many relevant aspects of an automobile such as stability, comfort and fuel consumption at high cruising speeds. The flow around the vehicles is characterized by high turbulent and three dimensional flow separations and there is a growing need for more insight into the physical features of these dynamical flows. The CFD (Computational Fluid Dynamics) analysis is used to find the parameter in the automobile industry. The air flow over ground vehicle is analyzed and coefficient of drag is calculated using CFD (Ansys Fluent). For this calculation, Ahmed body (simplified car body) as ground vehicle is considered which is commonly used as test case in industry. The Ahmed body is made up of a round front part, a movable slant plane placed in the rear of the body to study the separation phenomena at 25° and 35° angles. Aerodynamic drag is one of the main obstacles to accelerate a solid body when it moves in the air. About 50 to 60% of total fuel energy is lost only to overcome this adverse aerodynamic force. To win a race, which may be decided by fraction of second, the racing cars need a faster acceleration, which is possible by reducing the drag force by optimizing its shape to ensure stream-lining or reducing the separation. By adding vortex generators on the roof and extending the rear body of the car aerodynamically which could reduce the drag of the vehicle by 25% which further improves the fuel efficiency of the vehicle. The amount of grip available in the tires along with aerodynamic drag and engine power set the theoretical limits for the vehicle's velocity around the track, especially in cornering and it is thus of particular interest when designing a vehicle to increase this grip while keeping drag to a minimum. By adding a pair of flaps to a spoiler its aerodynamic downforce can be improved and additional downforce can be generated while cornering and braking by an actuating mechanism which closes the gap between the flaps. Also leading edge slats are also added to delay the separation of the slack side of the spoiler which reduces the aerodynamic drag at high angle of attack.

**Key words:** External Aerodynamics, Drag Co-efficient, Ahmed Body, Drag Forces, CFD Simulation

## I. INTRODUCTION

A real-life automobile is very complex shape to model or to study experimentally. However, the simplified vehicle shape employed by Ahmed. (1984) generates fully three-dimensional regions of separated flow which may enable a better understanding of such flows. Ahmed performed a series of wind-tunnel experiments in order to examine the wake structure around typical automobile geometries. The study focused on the time averaged structure obtained from

visualizations of flow in the wake region for smooth quarter scale automobile models.

The external aerodynamics of a car determines many relevant aspects of an automobile such as stability, comfort and fuel consumption at high cruising speeds. Several simple generic reference models have been proposed in the past to experimentally investigate the automotive aerodynamics and isolate relevant flow phenomena.

The Ahmed body is a simplified car used in automotive industry to investigate the influence of the flow structure on the drag. The external aerodynamics of the car determines many relevant aspects of an automobile such as stability, comfort and fuel consumption at high cruising speeds. The flow around the vehicles is characterized by high turbulent and three dimensional flow separations and there is a growing need for more insight into the physical features of these dynamical flows.

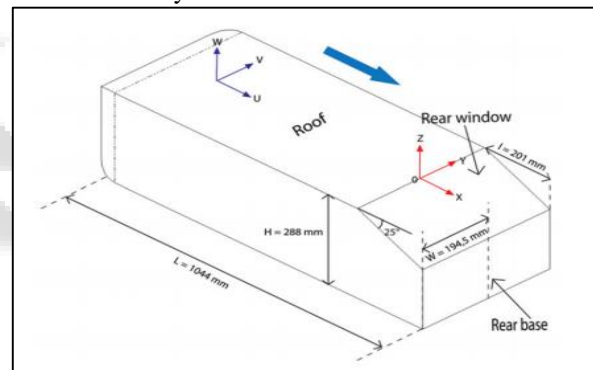


Fig. 1: Ahmed body

The use of Computational Fluid Dynamics (CFD) codes by the engineering community to predict aerodynamic flow around ground vehicles has increased dramatically in the last few years. This rise in interest and use has resulted from improvements in the predictive capabilities of codes reductions in the cost of computing technology and inflation of the costs to perform experiments and to maintain experimental facilities. Most industrially relevant geometries are usually defined in the CAD environment and must be translated and cleaned up to generate water-tight surfaces for simulations using the standard body-fitted approach. This process is very tedious and time consuming. In addition, during this process small details are usually eliminated and overlapping surface patches are trimmed. A smooth water-tight surface mesh is then made which serves as a boundary condition for the volume mesh. There are mainly two types of approaches in volume meshing, structured and unstructured meshing. In structured meshing, the governing equations are transformed into the curvilinear coordinate system aligned with the surface. It is trivial for simple shapes, however, it becomes extremely inefficient

and time consuming for complex geometries. In the unstructured approach, there is no transformation involved for governing equations. The integral form of governing equations is discretized and either a finite-volume or finite-element scheme is used. The information regarding the grid is directly incorporated into the discretization. Unstructured grids are in general successful for complex geometries. However, the quality of these grids deteriorates as the shapes become more complex. In addition, there is large computational overhead owing to a large number of operations per node and low accuracy in combination with the low-order dissipative spatial discretization

## II. OBJECTIVES

- 1) To make the analysis and comparison between the CFD simulation with the previous experimental result for validation. Different drag reduction mechanism to be investigated to reduce the drag coefficient of Ahmed body.
- 2) To choose optimized model for drag reduction mechanism for the Ahmed body based on CFD simulation.
- 3) The Drag Coefficient was evaluated using the following expression

$$C_d = F_d / (2 \rho A V^2)$$

Where  $C_d$  = Drag coefficient

$F_d$  = Drag Force, N

$\rho$  = Density of Air,  $kg/m^3$

$A$  = Frontal Area,

## III. AHMED BODY VALIDATION CASES

The Ahmed body validation was carried out by varying the rear-ramp angle.

- Validation Case 01 – Ramp Angle = 25 degree
- Validation Case 02 – Ramp Angle = 35 degree

### A. Validation Case – 01

Drag coefficient variation over the Reynolds Number variation for the Ahmed Body with the Rear Ramp (Slant) angle of 25 degree had been plotted in figure.

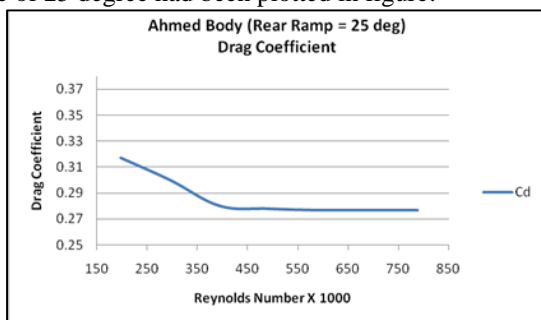


Fig. 1: Velocity Contours validation case -01

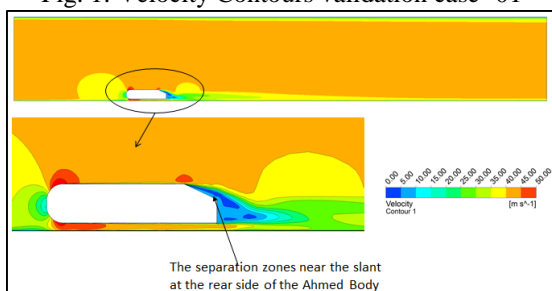


Fig. 2: Velocity Contours validation case -01

### B. Validation Case – 02

In similar with the Ramp Angle of 25 degrees case, a sharp variation of drag coefficient was observed for the low Reynolds number and remains nearly uniform for the higher Reynolds number cases shown in figure.

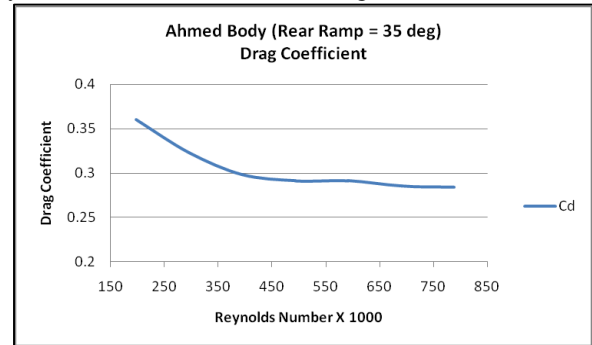


Fig. 3: Velocity Contours validation case -02

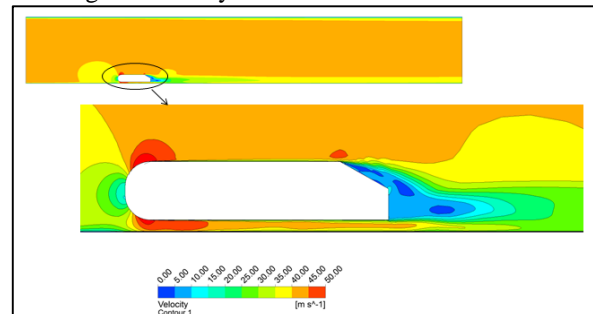


Fig. 4: Velocity Contours validation case -02

## IV. RESULT COMPARISON

The experimental value 0.260 are taken from journal of wind engineering and industrial aerodynamic 96(2008) 1207-1217.

Ramp Angle=35°		
Experiment	CFD	% Difference
0.260	0.284	-8%

Table 1: Result

- 1) The CFD simulations over predict Drag coefficient by 8% an brief study will be made to identify the potential areas to improve the results to meet the predictions from experiment
- 2) Improving grid refinement near the walls for better prediction of Skin-friction drag
- 3) Improving grid refinement in the wake region for better prediction of Pressure Drag
- 4) The reduction of vehicle drag for the increase in Reynolds number had been predicted using CFD simulation.
- 5) The drag prediction approach with the help of Reynolds Averaged Naiver Stokes (RANS) formulation with two equation model of K-omega turbulence model produced results that were comparable to the experimental data.

## V. DRAG REDUCTION MECHANISM OF AHMED BODY

The reduction of drag in road vehicles has led to increases in the top speed of the vehicle and the vehicle's fuel efficiency, as well as many other performance characteristics, such as handling and acceleration. The two main factors that impact drag are the frontal area of the vehicle and the drag

coefficient. The drag coefficient is a unit-less value that denotes how much an object resists movement through a fluid such as water or air. A potential complication of altering a vehicle's aerodynamics is that it may cause the vehicle to get too much lift. Lift is an aerodynamic force that flows perpendicular to the airflow around the body of the vehicle. Too much lift can cause the vehicle to lose road traction which can be very unsafe. Lowering the drag coefficient comes from streamlining the exterior body of the vehicle. Streamlining the body requires assumptions about the surrounding airspeed and characteristic use of the vehicle.

Aerodynamic drag is one of the main obstacles to accelerate a solid body when it moves in the air. About 50 to 60% of total fuel energy is lost only to overcome this adverse aerodynamic force. To win a race, which may be decided by fraction of second, the racing cars need a faster acceleration, which is possible by reducing the drag force by optimizing its shape to ensure stream-lining or reducing the separation. By adding vortex generators on the roof and extending the rear body of the car aerodynamically which could reduce the drag of the vehicle by 25% which further improves the fuel efficiency of the vehicle. The amount of grip available in the tires along with aerodynamic drag and engine power set the theoretical limits for the vehicle's velocity around the track, especially in cornering and it is thus of particular interest when designing a vehicle to increase this grip while keeping drag to a minimum. By adding a pair of flaps to a spoiler its aerodynamic downforce can be improved and additional downforce can be generated while cornering and braking by an actuating mechanism which closes the gap between the flaps. Also leading edge slats are also added to delay the separation of the slack side of the spoiler which reduces the aerodynamic drag at high angle of attack.

In order to reduce the drag from the vehicle, the following four configurations were studied. CFD simulations were conducted for the flow conditions corresponding to  $Re = 200,000$  to  $Re = 450,000$  at an interval of 50,000. Hence the impact of such drag reduction modifications could be studied for various vehicle speeds.

- Configuration A : Bottom Spoiler
- Configuration B: Rear Rectangular Spoiler
- Configuration C: Rear Slice
- Configuration D: Diffuser

A. Base Model

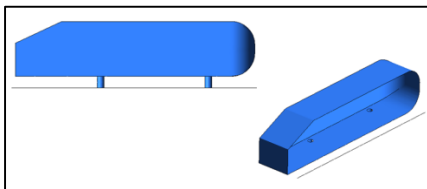


Fig. 5: Base model

The Base Model shown in figure without any drag reduction mechanism had a rear slant and simple horizontal surface at the bottom as can be observed.

1) Configuration A – Rectangular Spoiler at Bottom of Rear Side:

In order to minimize the local negative pressure in the downstream of the vehicle shown in figure a spoiler was placed at the bottom surface. This was expected to circulate

more air from the bottom of the vehicle to the downstream. With the reduction of negative pressure at the rear, the overall pressure difference across the vehicle would reduce and subsequently the reduction in drag coefficient.

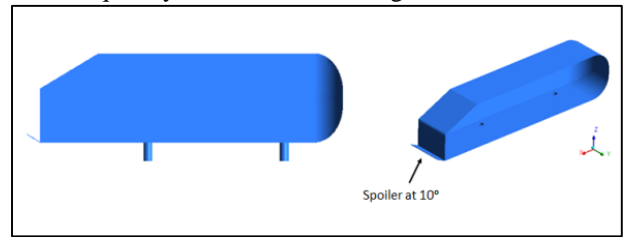


Fig. 6: Rectangular Spoiler at Bottom of Rear Side

2) Configuration B – Rectangular Spoiler at rear side

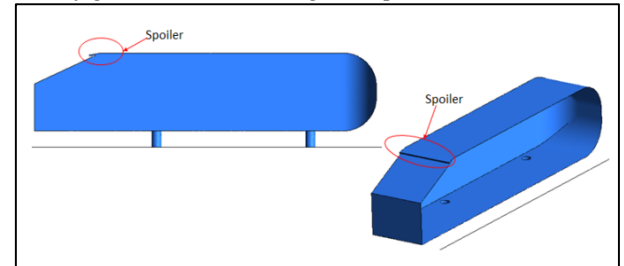


Fig. 7: Rectangular Spoiler at rear side

In another approach shown in figure 5.3 the Configuration B was created by introducing the Spoiler at the Rear Slant. The reasoning for this was reducing the flow separation that were occurring in the Base Model Ahmed Body at the rear slant position. Even though the flow separation was expected in the Configuration B – after introducing the Spoiler - the delay in flow separation was could result in lesser drag coefficient.

3) Configuration C – Rear slice at bottom side

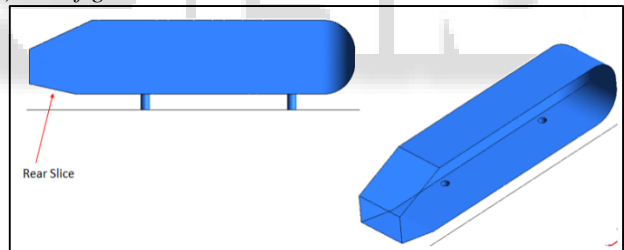


Fig. 8: Rear slice at bottom side

In Configuration C shown in figure a diverging slice was introduced at the rear bottom side of the vehicle with an objective to divert the flow towards the downstream of the vehicle. This flow pattern as discussed earlier would reduce the drag coefficient by the reduction of the negative pressure in these regions. The diverging angle was chosen with a consideration to smoothly direct the flow from the vehicle bottom to the rear portion of vehicle.

4) Configuration D – Diffuser at rear side-

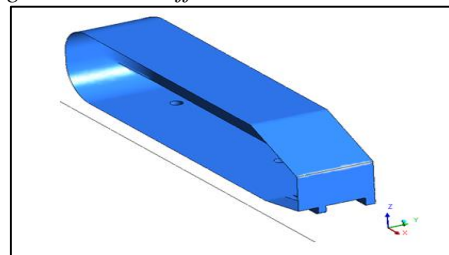


Fig. 9: Diffuser at rear side

In an improvised model of Configuration C shown in figure the guided channels – known as Diffusers – were placed at the rear bottom of the vehicle for the Configuration D.

5) Drag coefficient of base model

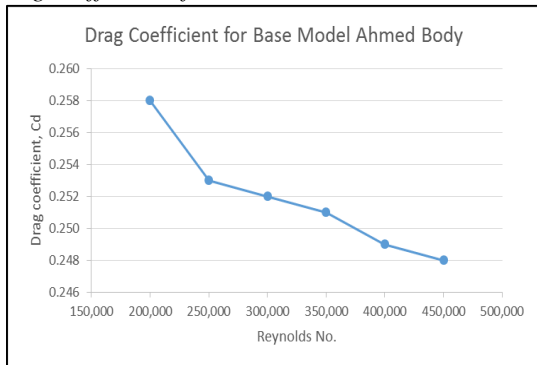


Fig. 10: Drag coefficient of base model

Reynolds No.	Base Model
200,000	0.258
250,000	0.253
300,000	0.252
350,000	0.251
400,000	0.249
450,000	0.248

Table 2: Result

6) Drag coefficient of configuration A-

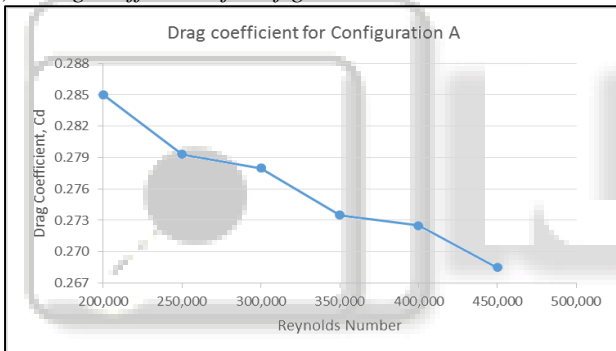


Fig. 11: Drag coefficient of configuration

Reynolds No.	Drag Coefficient		% Change in Drag Coefficient for Configuration A
	Base Model	Configuration A	
200,000	0.258	0.285	10.5%
250,000	0.253	0.279	10.4%
300,000	0.252	0.278	10.3%
350,000	0.251	0.274	9.0%
400,000	0.249	0.273	9.4%
450,000	0.248	0.269	8.3%

Table 3: Result

7) Drag coefficient of configuration B

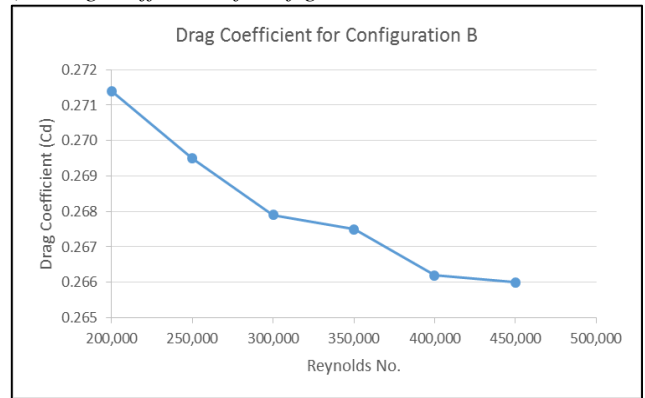


Fig. 12: Drag coefficient of configuration

Reynolds No.	Drag Coefficient		% Change in Drag Coefficient for Configuration B
	Base Model	Configuration B	
200,000	0.258	0.271	5.2%
250,000	0.253	0.270	6.5%
300,000	0.252	0.268	6.3%
350,000	0.251	0.268	6.6%
400,000	0.249	0.266	6.9%
450,000	0.248	0.266	7.3%

Table 4: Result

8) Drag coefficient of configuration C

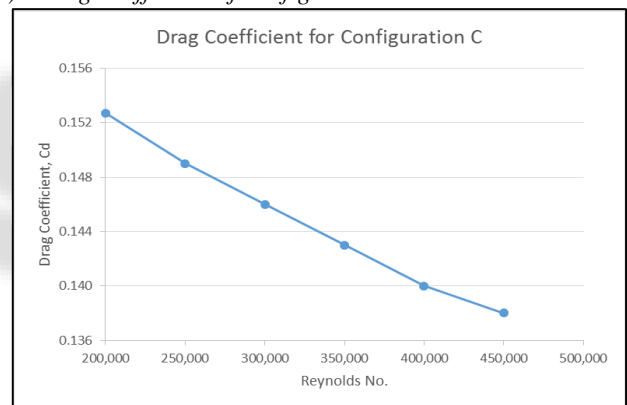


Fig. 13: Drag coefficient of configuration

Reynolds No.	Drag Coefficient		% Change in Drag Coefficient for Configuration C
	Base Model	Configuration C	
200,000	0.258	0.153	-40.8%
250,000	0.253	0.149	-41.1%
300,000	0.252	0.146	-42.1%
350,000	0.251	0.143	-43.0%
400,000	0.249	0.140	-43.8%
450,000	0.248	0.138	-44.4%

Table 5: Result



9) Drag coefficient of configuration D

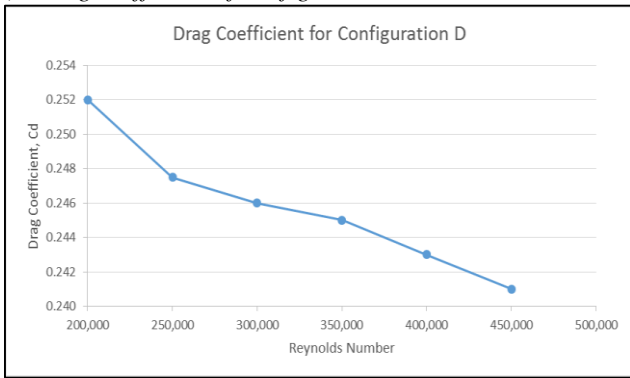


Fig. 14: Drag coefficient of configuration D

Reynolds No.	Drag Coefficient		% Change in Drag Coefficient for Configuration D
	Base Model	Configuration D	
200,000	0.258	0.252	-2.3%
250,000	0.253	0.248	-2.2%
300,000	0.252	0.246	-2.4%
350,000	0.251	0.245	-2.4%
400,000	0.249	0.243	-2.4%
450,000	0.248	0.241	-2.8%

Table 6: Result

10) Result comparison of all configurations

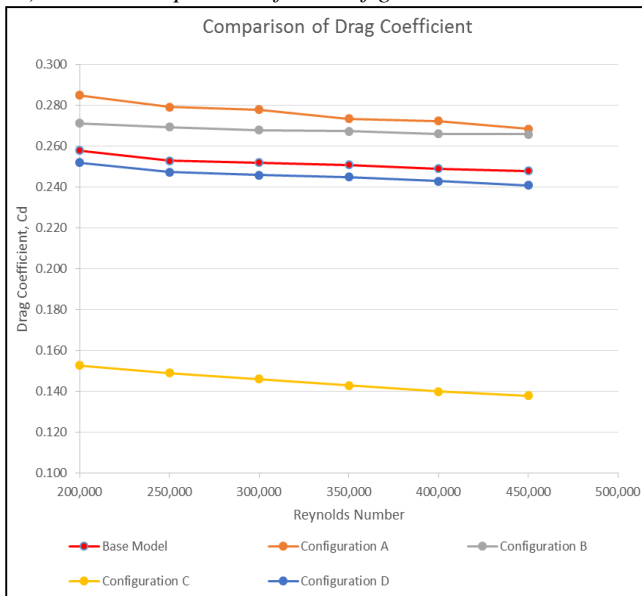


Fig. 15: Result comparison of all configurations

Reynolds No.	Base Model	Conf. A	Conf. B	Conf. C	Conf. D
200,000	0.258	0.285	0.271	0.153	0.252
250,000	0.253	0.279	0.270	0.149	0.248
300,000	0.252	0.278	0.268	0.146	0.246
350,000	0.251	0.274	0.268	0.143	0.245
400,000	0.249	0.273	0.266	0.140	0.243
450,000	0.248	0.269	0.266	0.138	0.241

Table 7: Result

VI. CONCLUSION

- 1) The drag coefficient for the Base Model (without any drag reduction mechanisms) predicted from these simulations were within 5% difference from the experimental results. This indicates that the CFD

simulations methods that were adopted for these projects resulted in prediction of results that were close to experimental data.

- 2) With the increase in Reynolds Number (and the subsequent increase in flow velocity) the drag coefficient was observed to be decreasing. This trend was noted for all the configurations.
- 3) When the Bottom Spoiler (Configuration A) was attached to the Ahmed Body vehicle, the drag was observed to be increasing (~10%) as compared to the Base Model. This trend was consistent for all the flow conditions that were studied. So, it can be concluded that this Bottom Spoiler was not optimized for the vehicle drag reduction.
- 4) The Rear Rectangular Spoiler (Configuration B) also resulted in high drag coefficient as compared to the Base Model. However, this drag reduction mechanism resulted in relatively lesser drag coefficient in comparison to Configuration A.
- 5) Of the four drag reduction configurations that were investigated in this project work, the Rear Slice (Configuration C) resulted high drag reduction – as much as 45% as compared to the Base Model. The drag reduction was consistent for all the flow conditions. The Rear Slice ensured that the flow from the bottom of the vehicle was circulated to the rear end of the vehicle. Thus the drag was reduced significantly.
- 6) In Configuration D (Diffuser) the drag coefficient were remained almost unchanged as compared to the Base Model.

REFERENCES

- [1] J.D. Yau “Aerodynamic vibrations of a maglev vehicle running on flexible guideways under oncoming wind actions” Journal of Sound and Vibration 329 (2010) 1743–1759
- [2] Makoto Tsubokura , Takuji Nakashima b, Masashi Kitayama c, Yuki Ikawa , Deog Hee Doh d, Toshio Kobayashi e “Large eddy simulation on the unsteady aerodynamic response of a road vehicle in transient crosswinds” International Journal of Heat and Fluid Flow 31 (2010) 1075–1086
- [3] Ehab Fares “Unsteady flow simulation of the Ahmed reference body using a lattice Boltzmann approach” Computers & Fluids 35 (2006) 940–950
- [4] Charles-Henri Bruneau a, Emmanuel Creusé b, Delphine Depeyras a, Patrick Gilliéron c, Iraj Mortazavi a “Coupling active and passive techniques to control the flow past the square back Ahmed body” Computers & Fluids 39 (2010) 1875–1892
- [5] Daniel G. Hyams, Kidambi Sreenivas, Ramesh Pankajakshan, D. Stephen Nichols, W. Roger Briley, David L. Whitfield “Computational simulation of model and full scale Class 8 trucks with drag reduction devices” Computers & Fluids 41 (2011) 27–40
- [6] Eric Serre, Matthieu Minguez, Richard Pasquetti, Emmanuel Guilmineau, Gan Bo Deng, Michael Kornhaas, Michael Schäfer, Jochen Fröhlich, Christof Hinterberger, Wolfgang Rodi, “On simulating the turbulent flow around the Ahmed body: A French German collaborative evaluation of LES and DES” Computers & Fluids 78 (2013) 10–23

- [7] Emmanuel Guilmineau “Computational study of flow around a simplified car body” *Journal of Wind Engineering and Industrial Aerodynamics* 96 (2008) 1207–1217
- [8] Simon Watkins, Gioacchino Vio “The effect of vehicle spacing on the aerodynamics of a representative car shape” *Journal of Wind Engineering and Industrial Aerodynamics* 96 (2008) 1232–1239
- [9] Mahmoud Khaled , Hicham El Hage, Fabien Harambat , Hassan Peerhossaini “Some innovative concepts for car drag reduction: A parametric analysis of aerodynamic forces on a simplified body” *J. Wind Eng. Ind. Aerodyn.* 107–108 (2012) 36–47
- [10] Bahram Khalighi, Shailesh Jindal b, Gianluca Iaccarini “Aerodynamic flow around a sport utility vehicle Computational and experimental investigation” *J. Wind Eng. Ind. Aerodyn.* 107–108 (2012) 140–148
- [11] Siniša Krajnović, João Fernandes “Numerical simulation of the flow around a simplified vehicle model with active flow control” *International Journal of Heat and Fluid Flow* 32 (2011) 192–200
- [12] D. Rubinstein and R. Hitron “A detailed multi-body model for dynamic simulation of off-road tracked vehicles” *Journal of Terra mechanics* 41 (2004) 163–173
- [13] Korkischko and J. R. Meneghini “Experimental Investigation And Numerical Simulation Of The Flow Around An Automotive Model: Ahmed Body” 19th International Congress of Mechanical Engineering November 5-9, 2007

